HYDROGEOLOGIC MODELING OF FLOW WITHIN SULFATE-REDUCING BIOREACTORS: IMPLICATIONS FOR SYSTEM DESIGN AND PERFORMANCE[1]

Robert C. Waddle[2] and Greg A. Olyphant

Abstract: Sulfate-reducing bioreactor cells (SRBCs) are one alternative for the mitigation of acid mine drainage (AMD) at abandoned mine land sites. More than three years of monitoring three SRBCs in southwestern Indiana indicates that they do not perform as optimally as hoped and can even fail before the end of their expected lifespan. A better understanding of how the internal flow of water in SRBCs is influenced by their size, morphology, and rates and distributions of inflow and outflow of AMD could help explain performance complications and ultimately lead to more efficient design criteria. To address this issue, hydrogeologic models for each SRBC were developed by using interpolation methods that incorporated engineering plans and field surveys. A three-dimensional, groundwater-flow model was then used to characterize the flow regime that would result under conditions reflected by the SRBC designs at initial stages of deployment. Results indicate that the geometric configuration and inflow rates for each bioreactor lead to fundamentally different flow regimes. Particle-tracking analyses indicated transit times that ranged from 72 days to less than 1 day. The extension of collection pipes along the base of a larger SRBC experiencing high surficial AMD inflow succeeded in drawing surface water down into the reactive substrate. However, in doing so the distance of subsurface travel from inflow to pipe network was shortened, resulting in smaller simulated transit times. Longer transit times were simulated for a moderately sized, low-discharge SRBC, but the addition of a high permeable woodchip layer to help promote flow into the system reduced the residence time of the AMD within the reactive substrate. Jointed pipes within a small bioreactor promoted flow throughout the substrate, but enhanced inflow at pipe junctions led to rapid transit times that may also have undermined bioreactor performance. Future designs of SRBCs should aim to optimize initial hydrologic performance as well as account for potential changes in hydraulic properties owing to physical-chemical reactions.

Additional Key Words: Acid mine drainage, groundwater-flow modeling

---

[1] Paper was presented at the 2012 National Meeting of the American Society of Mining and Reclamation, Tupelo, MS ***Sustainable Reclamation*** June 8 – 15, 2012. R.I. Barnhisel (Ed.) Published by ASMR, 3134 Montavesta Rd., Lexington, KY 40502.

[2] Robert Waddle is a Ph.D. Candidate, Department of Geological Sciences and the Center for Geospatial Data Analysis, Indiana University, Bloomington, IN 47405, and Greg Olyphant is a professor, Department of Geological Sciences and the Center for Geospatial Data Analysis, Indiana University, Bloomington, IN 47405.

Proceedings America Society of Mining and Reclamation, 2012 pp 500-519
DOI: 10.21000/JASMR12010500
http://dx.doi.org/10.21000/JASMR12010500

Introduction

Sulfate-reducing bioreactor cells (SRBCs) are currently being used in the treatment of acid mine drainage (AMD) originating from abandoned coal mines. They are promising as a cost-effective mitigation tool, but very little is known about their long-term performance in field situations. Complications can arise from both initial design criteria as well as from physical-chemical changes that occur as a result of geochemical reactions over time. Ongoing monitoring of three SRBCs in southwestern Indiana from the very initial phase of construction shows mixed results related to the geometric and hydraulic engineering design. Further complications arise as a result of geochemical evolution within bioreactors, which can alter the internal flow dynamics (Branam et al., 2012). Documentation of how engineering designs influence groundwater flow through bioreactors as well as temporal changes in matrix distribution (the chemical alterations that can change hydraulic conductivity) could help avoid performance issues for future SRBCs. In a companion paper, Branam et al. (2012) discusses the geochemical characteristics of these bioreactors. The purpose of this paper is to document modeling studies of how the flow of groundwater in SRBCs in the initial phase of deployment is conditioned by their size, morphology, and the rates and methods of AMD inflow and outflow. Three-dimensional (3-D) geologic models were created to represent each of the three bioreactors that were designed and constructed by personnel of the Indiana Department of Natural Resources-Division of Reclamation (IDNR-DOR) to treat AMD seeps in southwestern Indiana. The models included the respective hydrogeomorphological environments and a representation of the pipe network configurations emplaced within each bioreactor to manipulate the hydrology within each system. A groundwater flow model was then implemented at each site in order to simulate theoretical hydrologic conditions and give information on the role of geometry and internal piping on the flow throughout the system. Results indicate that flow fields can be complex inside the bioreactors and more consideration should be given to all aspects of the initial design and implementation.

Hydrogeologic Model

Mathematical Model

The model used to study flow through constructed bioreactors is a 3-D finite-difference model based on that of Freeze (1971). The model is capable of incorporating the hydrogeological

complexity that exists within SRBCs. Of particular importance is the explicit incorporation of 3-D geometry and the ability to represent flow into and out of internal piping networks as specified flux boundary conditions. The model also allows explicit treatment of both saturated and unsaturated groundwater flow that may be important in situations where the water table within the bioreactor is fluctuating over time.

Freeze (1971) expressed the combined equations for saturated flow (Jacob, 1940) and unsaturated flow (Richards, 1931) in terms of the pressure head (Ψ); where $\Psi > 0$ in the saturated zone, $\Psi = 0$ at the water table, and $\Psi < 0$ (tension head) in the unsaturated zone. In its most general form, the equation is as follows (Freeze 1971, p. 349):

$$\frac{\partial}{\partial x}\left[\frac{g}{\mu}\rho^2 k_x(\Psi)\frac{\partial \Psi}{\partial x}\right] + \frac{\partial}{\partial y}\left[\frac{g}{\mu}\rho^2 k_y(\Psi)\frac{\partial \Psi}{\partial y}\right] + \frac{\partial}{\partial z}\left[\frac{g}{\mu}\rho^2 k_z(\Psi)\left\{\frac{\partial \Psi}{\partial z} + 1\right\}\right] = \left[\frac{\rho\theta(\Psi)}{n}\{\alpha' + n\beta'\} + \rho C(\Psi)\right]\frac{\partial \Psi}{\partial t} \quad (1)$$

where x, y, and z are the coordinate directions [cm], t is time [s], Ψ is the pressure head [cm of water], ρ is the mass density of water [$\approx$ 1.0 g/cm^3], g is the acceleration due to gravity [$\approx$ 980 cm/s^2], μ is the dynamic viscosity of water [$\approx$ 0.018 g/cm·s], θ is the volumetric moisture content [decimal fraction], n is the porosity of the porous media [decimal fraction], $C(\Psi)$ (= $d\theta/d\Psi$) is the specific moisture capacity of the porous media [cm^{-1}], and $\alpha' = \alpha\rho g$ and $\beta' = \beta\rho g$, where α and β represent the vertical compressibilities of the porous media and water [Pa^{-1}], respectively. The parameters $k_x(\Psi)$, $k_y(\Psi)$, $k_z(\Psi)$ are the pressure-head-dependent intrinsic permeabilities of the porous media [cm^2] measured in the direction of the three principle axes x, y, and z, respectively. Note that the hydraulic conductivity K_s [cm/s] in the direction s, ($s = x,y,z$), is related to the specific permeability by $K_s = k_s\rho g/\mu$. The pressure-head-dependent parameters $C(\Psi)$ and $K_s(\Psi)$ are the result of incorporating flow in the unsaturated zone.

To solve the governing equation, an effective means of calculating the pressure-head-dependent parameters is needed. We adopted the now-standard approach of Mualem (1976) and van Genuchten (1980), who derived expressions representing the average values of the so-called characteristic curves. The functional relationships are as follows:

$$\Theta = \frac{\theta - \theta_r}{\theta_s - \theta_r} = \left(\frac{1}{1 + (a|\Psi|)^N}\right)^m \quad (2)$$

where Θ is the relative soil-water content , θ_s ($\approx n$) and θ_r are the saturated and residual moisture contents, respectively, and *a*, *N*, and *m* are fitting parameters describing the shape of the soil-water retention curve. The variable *m* is related to *N* by *m = 1-(1/N)*. By rearranging Eq. 2 and differentiating with respect to Ψ, an analytical expression for the specific moisture capacity can be derived (Boswell and Olyphant, 2007):

$$C(\Psi) = \frac{\partial\theta}{\partial\Psi} = \frac{mNa^N \cdot (\theta_s - \theta_r) \cdot |\Psi|^{N-1}}{[1 + (a|\Psi|)^N]^2}\left(\frac{1}{1 + (a|\Psi|)^N}\right)^{m-1} \quad (3)$$

Because θ is a function of Ψ, van Genuchten (1980) was able to express the characteristic curve for *K*(Ψ) as follows:

$$K(\Theta) = K_0\Theta^{1/2}\left[1 - \left(1 - \Theta^{1/m}\right)^m\right]^2, (0 < m < 1) \quad (4)$$

where K_0 is the saturated hydraulic conductivity [cm/s] and θ is computed from Ψ using Eq. 2. Note that hysteretical effects associated with wetting and drying curves for unsaturated flow were not considered in our models. We also did not distinguish between directional components of hydraulic conductivity except where permeability boundaries occurred within the porous media.

Solution Method

Eqs. (1-4) were solved numerically by discretizing the model domain into a "brick pile" using a block-centered nodal grid. In this way, the system of equations can be approximated in implicit finite-difference form (Freeze 1971, p. 351) and solved for Ψ at each grid cell, subject to any imposed configuration of boundary conditions, including a specified flux or fixed-head. The models for bioreactor performance were run in transient mode, subject to prescribed inflows but with no other forcing such as changes in prevailing weather. Other details of how boundary conditions were defined for each study bioreactor are provided in the sections below. The initial conditions for the transient simulations were 3-D distributions of hydraulic head values based on observed conditions for each modeled SRBC (e.g., surveyed water table elevation). The model, which employs line successive over-relaxation with a tolerance of 0.01 cm, is written in Fortran and can be executed on a desktop computer.

Model output is in the form of a 3-D grid of pressure-head values (a value for each cell in the finite-difference grid) for each time-step of the model simulation. From this information, all other pertinent hydrologic information can be extracted, including the elevation of the water table at each x and y vertical prism, profiles of soil moisture where unsaturated conditions occur, and a 3-D representation of the flow field, which is generated by resolving the three spatial components of the specific discharge. Post processing to extract such information is done mostly within Fortran and Matlab programming environments. Particle tracking and transit time calculations were also made using the resultant flow velocities (specific discharge/porosity) from the model simulations. The computational methods used for these calculations are based on those outlined in Pollock (1988).

Hydrogeologic models for the three bioreactors were created by combining onsite transit surveys with digital engineering designs developed by personnel of the IDNR-DOR. All data (point data from surveys and digital line graph data) were georeferenced within ESRI's ArcGIS software package. The digital line graph data (digital topographic contours) represented the surficial configurations of each site both before construction and after the SRBCs were installed. Inverse distance weighting interpolation models within ArcGIS were used to interpolate continuous raster surfaces from the control data. Computer algorithms written in Matlab and Fortran used the raster layers (generated by ArcGIS) to construct the 3-D finite-difference grids ("brick piles") representing each SRBC. Each grid cell of the 3-D model was assigned spatial coordinates (row, column, layer) and a sediment identification code. The sediment identification codes were then assigned hydraulic properties for use in the groundwater-flow simulations. The hydraulic properties for the reactive substrate (Table 1) in all three hydrogeologic models were based on values that were recommended for highly permeable porous material by Schaap et al. (2000).

Table 1. Hydraulic parameters used in the hydrogeologic modeling.

Hydraulic Parameters				
K_0 (cm/s)	a (cm^{-1})	N	θ_s	θ_r
1.0E-02	0.035	3.18	0.375	0.053

Bioreactor Configurations

The three study bioreactors are located in southwestern Indiana, one near Augusta and the other two near Shoals (Fig. 1). The AMD flow rates and the geomorphological setting at each location are different. These differences led to three distinct engineering designs. Each bioreactor contains roughly the same composition of reactive substrate: hay (50% by volume), woodchips (30% by volume), garden compost (10% by volume), and crushed limestone (10% by volume). Note, however, that the Midwestern bioreactor used straw in place of hay.

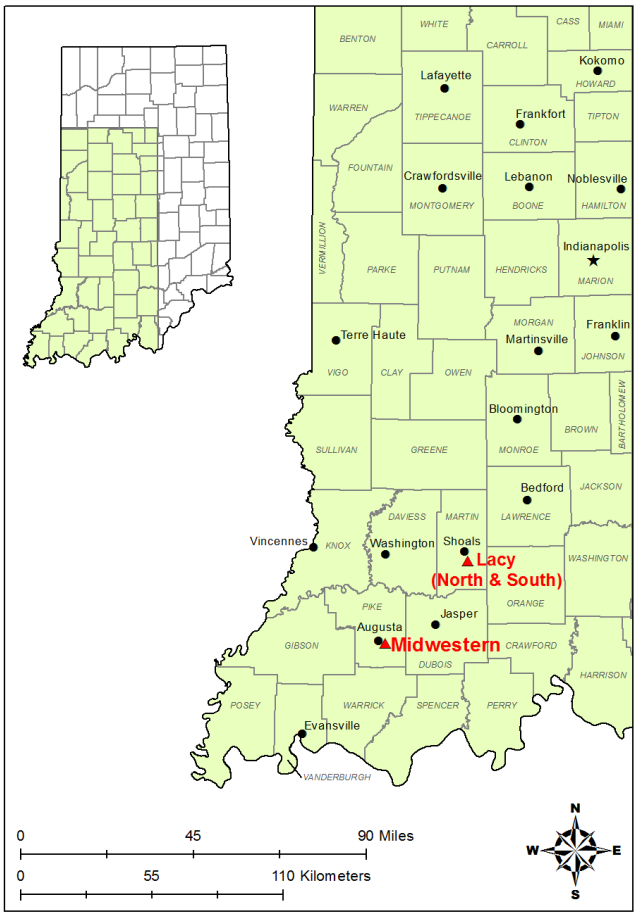

Figure 1. Map of southwestern Indiana showing the locations of study areas.

The Lacy North and Lacy South SRBCs were constructed in June 2009 at the site of the Cross-Roads Mine, a mine that has been abandoned for over 100 years. Acid mine drainage emerges at each SRBC location in the form of seeps along the periphery of the abandoned mine. Both SRBCs were designed as “up flow” treatment systems, where raw AMD enters at the base and is discharged through a collection pipe located near the surface.

Lacy North

The Lacy North bioreactor is positioned within a small preexisting valley that was excavated to create a basin enclosed by clay-rich soil. A levee was constructed on the downstream end of the basin to hold the substrate in place. The bioreactor has an average length of 18 m and width of 6 m. The average thickness of the reactive substrate is 1.5 m, and lies on top of a 0.9-m-thick layer of woodchips. Acid mine drainage enters through two separate seeps located at the base of the northeast end of the bioreactor and is discharged through a standpipe at the southwest end. The standpipe was slotted to fix the water table within the bioreactor to approximately 2.4 m above its base at the discharge end. The average total AMD flow rate is approximately 6 L/min.

The hydrogeologic model for the Lacy North SRBC consisted of nine layers at the base, having a saturated hydraulic conductivity of 1.0×10^{-1} cm/s to represent the woodchips, followed by 15 layers with $K_0 = 1.0 \times 10^{-2}$ cm/s to represent the reactive material. The clay grid cells surrounding the SRBC (Fig. 2), including those representing the dam, were assumed to be impermeable. The spatial resolution ($\Delta x = \Delta y = \Delta z$) for the Lacy North SRBC was set at 0.1 m. At this resolution, a 3-D grid with a total of 116 rows, 230 columns, and 33 layers was needed to accommodate the spatial extent of the SRBC. Some of the cells in the 3-D grid are outside the solution domain (e.g., they are in the air), but 391,392 cells were still subjected to numerical analysis.

The transient-flow simulation was implemented with the initial condition being a 3-D distribution of pressure-head values corresponding to a water-table elevation equal to that of the slotted standpipe. The model was run using a variable time step for six days. This duration, which included a total of 1,728 individual time-steps, was sufficient to develop a quasi-steady flow field within the model domain. Flow into the grid cell representing the standpipe (flow out of SRBC) was implemented within the groundwater-flow model as a constant flux across the sides of the cell (sink) equating to the corresponding measured outflow data. Inflow was assumed to be equal to the measured outflow. Observations made during construction indicated that one of the two seeps was about three times greater than the other, so flow of the larger seep was set to 75 percent of the total inflow in the model. Inflow at each seep grid location was implemented as a constant upward basal flux across the base of the cell.

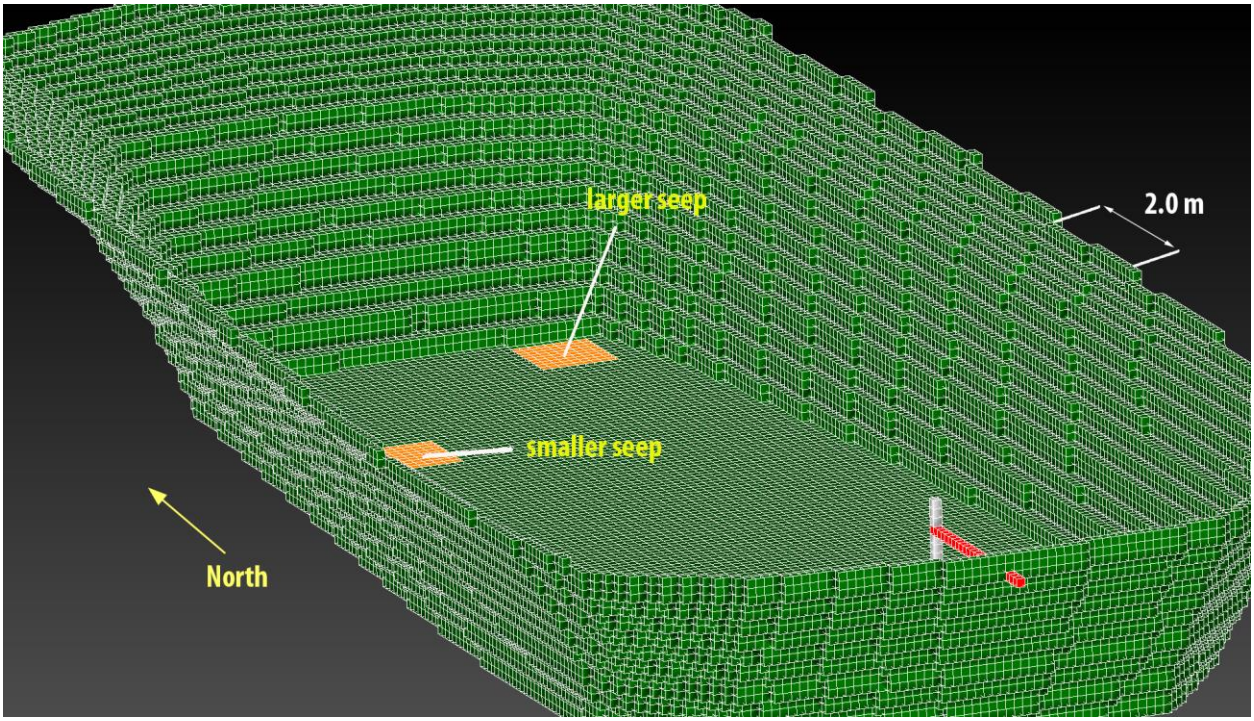

Figure 2. Three-dimensional illustration of the finite-difference grid of the surrounding impermeable clay sediment of the Lacy North SRBC. The orange cells represent the locations of the two AMD seeps. The white grid cells represent the outflow standpipe that collected groundwater for ultimate discharge through a pipe (red grid cells) leading to a settling pond. For reference, the larger seep is 0.9 m by 0.9 m.

Lacy South

The Lacy South bioreactor was constructed by digging a trench approximately 15 m long, 4 m wide, and 1.8 m thick. Acid mine drainage was collected up gradient of the SRBC and entered the system through a pipe network lying flat across the base of the bioreactor (Fig. 3). The AMD entering the SRBC occurred at an average rate of about 11 L/min. A parallel collection pipe extends above the basal pipe and was positioned at the top of the reactive substrate. The design called for water to enter the cell from perforations in the basal pipe then to migrate vertically through the substrate before entering the perforated upper pipe. The upper pipe ultimately discharged the collected water into a nearby drainage ditch. Lacy South is unique because it was completely underground below a 1.5-m-thcik clay-rich fill material.

The hydrogeologic model for the Lacy South SRBC was similar to that of Lacy North in that it consisted of the bioreactor substrate surrounded by low permeability clay. The space between grid nodes in the Lacy South SRBC was also chosen to be 0.1 m for all three spatial components.

At this resolution, it took a total of 37 rows, 181 columns, and 18 layers to accommodate the spatial extent of the SRBC. Altogether, 101,422 cells were subjected to numerical analysis.

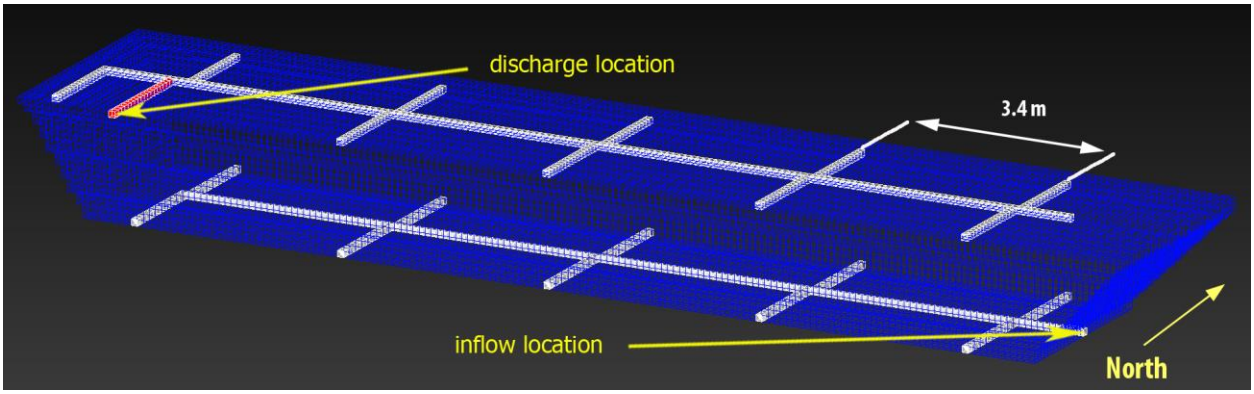

Figure 3. Three-dimensional illustration of the finite-difference grid of the Lacy South SRBC illustrating the reactive substrate and pipe networks. Impermeable clay grid cells surround the SRBC and are not shown here.

The transient flow simulation for Lacy South also consisted of six simulation days having a total of 1,728 variable time-steps. The initial condition was a 3-D distribution of pressure-head values corresponding to completely saturated conditions (water table at top of reactive substrate). The internal boundary conditions representing integrated volumetric flow through the pipe network (out of the basal pipe and into the surface pipe) was achieved by specifying equal constant fluxes across the faces of the grid cells representing pipes in such a proportion that they satisfied the integrated flux into and out of the SRBC. No-flow boundary conditions were imposed on all sides of the bioreactor, including top and bottom layers.

Midwestern

The Midwestern SRBC was constructed in August 2008 to treat AMD that emerges as a spring emitting from an abandoned underground mine (Midwestern #1 Mine). The spring has an average flow rate of 43 L/min. The bioreactor is designed as a “down flow” system, as the raw AMD enters at the surface and is ultimately discharged through a perforated collection pipe network located at the base of the cell (Fig. 4). The bioreactor cell is located within a valley that is on average 90 m long and 10 m wide. The inflow end is approximately 2 m deep and the base tapers upward towards the outflow end to a thickness of approximately 1 m. Water is ponded above the substrate much of the time. The depth of ponding is typically less than 0.5 m.

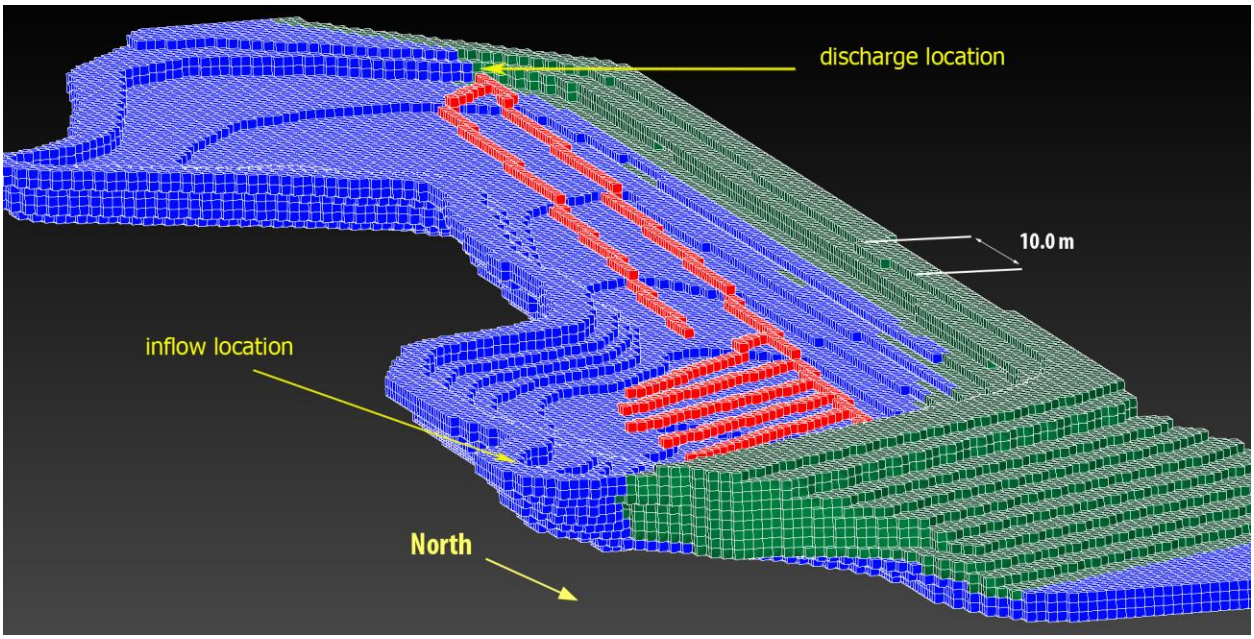

Figure 4. Three-dimensional illustration of the Midwestern SRBC finite-difference grid showing the alluvium (blue) beyond the reactive substrate (not shown), the constructed berm (green) to inhibit lateral leakage and the collection pipe network (red). Bedrock grid cells on the left side and beneath the alluvium were assumed to be impermeable boundaries. Water can enter anywhere along the pipe network and is ultimately discharged into a settling pond. For reference, each grid cell is 0.5 m along all sides.

The hydrogeologic model for the Midwestern SRBC consisted of four different sediment/rock types (bioreactor substrate, alluvium, clay, and bedrock). The preconstruction data were used to generate the base of the geologic model (alluvium and bedrock layers) that existed in the valley. These data were then combined with the post construction data depicting a perimeter levee consisting of clay (Fig. 4). The spatial resolution ($\Delta x=\Delta y=\Delta z$) was chosen to be 0.5 m. At this resolution, it took a total of 90 rows, 316 columns, and 13 layers to accommodate the spatial extent of the SRBC. A total of 124,050 grid cells were subjected to numerical analysis.

The perforated pipe network that lies at the base of the substrate was also distinguished within the finite-difference grid. As was the case with the Lacy South SRBC simulations, the integrated volumetric flow through the pipe network was achieved by specifying a constant flux across each face of each pipe grid cell that satisfied the measured discharge into and out of the SRBC. The initial condition was a 3-D distribution of pressure-head values corresponding to the average elevation of ponded water on top of the SRBC (determined from transit surveys).

Results of Numerical Simulations

The results of the numerical simulations of flow show that the hydrogeologic framework and pipe-network design have significant effects on the flow patterns and transit times of water in SRBCs. Data representing hydrologic attributes and simulated flow dynamics are shown in Tables 2 and 3 and are the focus of the following discussion.

Table 2. Measured discharges (inflow/outflow) and holding capacities of the three modeled SRBCs and simulated groundwater-flow vector magnitudes, where N_v is the total number of vectors processed for each respective SRBC.

	Average Discharge (L/min)	Storage Capacity (m^3)	Flow Vector Magnitude (cm/day)				
			N_v	Mean	Median	Maximum	Minimum
Lacy North	6	133	391,392	18.5	4.5	1860	0
Lacy South	11	38.0	101,422	75.0	65.6	525	0
Midwestern	43	1367	28,506	142	82.5	2490	0

Table 3. Simulated transit times based on particle tracking using resultant flow vectors from the hydrogeologic model. N_s is the total number of starting locations processed for each respective SRBC and is based their respective AMD inflow distributions.

	Lacy North (N_s = 137)		Lacy South (N_s = 863)		Midwestern (N_s = 71)	
	Distance Traveled (m)	Transit Time (day)	Distance Traveled (m)	Transit Time (day)	Distance Traveled (m)	Transit Time (day)
Mean	14.4	54.1	2.19	2.10	31.8	15.5
Median	13.6	53.8	2.32	2.06	31.5	15.0
Maximum	17.7	71.6	3.91	11.4	38.1	22.3
Minimum	12.5	45.7	1.70	0.91	28.7	11.9

Lacy North

The average simulated rate of flow within the Lacy North SRBC was 18.5 cm/day. The highest simulated flow rates occurred near the seep inflow locations and at the standpipe outflow location (Figure 5). As expected, the flow within the more permeable woodchip layer was consistently higher than the flow within the substrate. There is an area of lower flow in between the inflow and outflow locations, where the flow lines become roughly parallel, but there are significant vertical components of flow at the inflow and outflow locations (Fig. 5b).

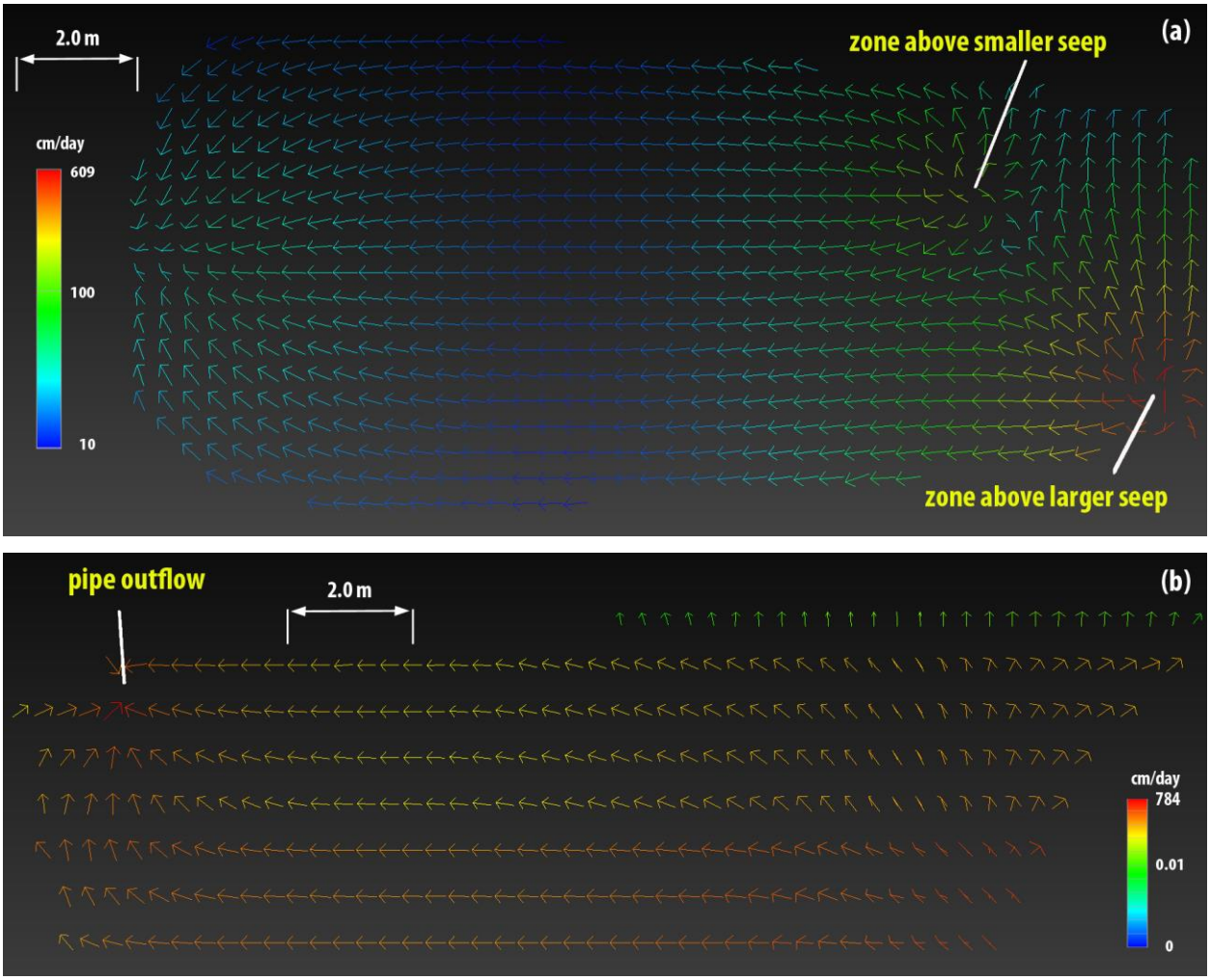

Figure 5. Maps of simulated flow vectors. (a) Flow vectors for Lacy North SRBC at layer 6 of the hydrogeologic model. This was 0.6 m above the base of the SRBC and is positioned within the higher permeability material (woodchips). (b) Flow vectors for Lacy North SRBC along a vertical cross section (VE=2X) that intersects the outflow pipe. Note that for clarity, only every fifteenth vector is shown in both (a) and (b). Each scale bar represents individual vector magnitudes (cm/day) and is logarithmic.

The computed particle paths for four different starting locations (Fig. 6) show that the path a particle takes depends on where it emanates from the area of seepage. For example, Path A (the minimum transit time which was 45.7 days) starts at a seepage location that is closest to the outflow pipe and exhibits a mostly linear path. Path B emanates from the side of the larger seep and it exhibits initial outward flow before finally heading more directly toward the outflow pipe. Finally, it should be noted that the tabulated transit times (Table 3) are for initial starting locations at each of the two seepage zones. The modeling indicates that there are cases where particles migrate most of the length of the SRBC through the woodchip layer and do not reach

the reactive substrate until near the outflow end. In the case of Path A, of the total computed transit time (45.7 days), only approximately 3.4 days are within the reactive substrate.

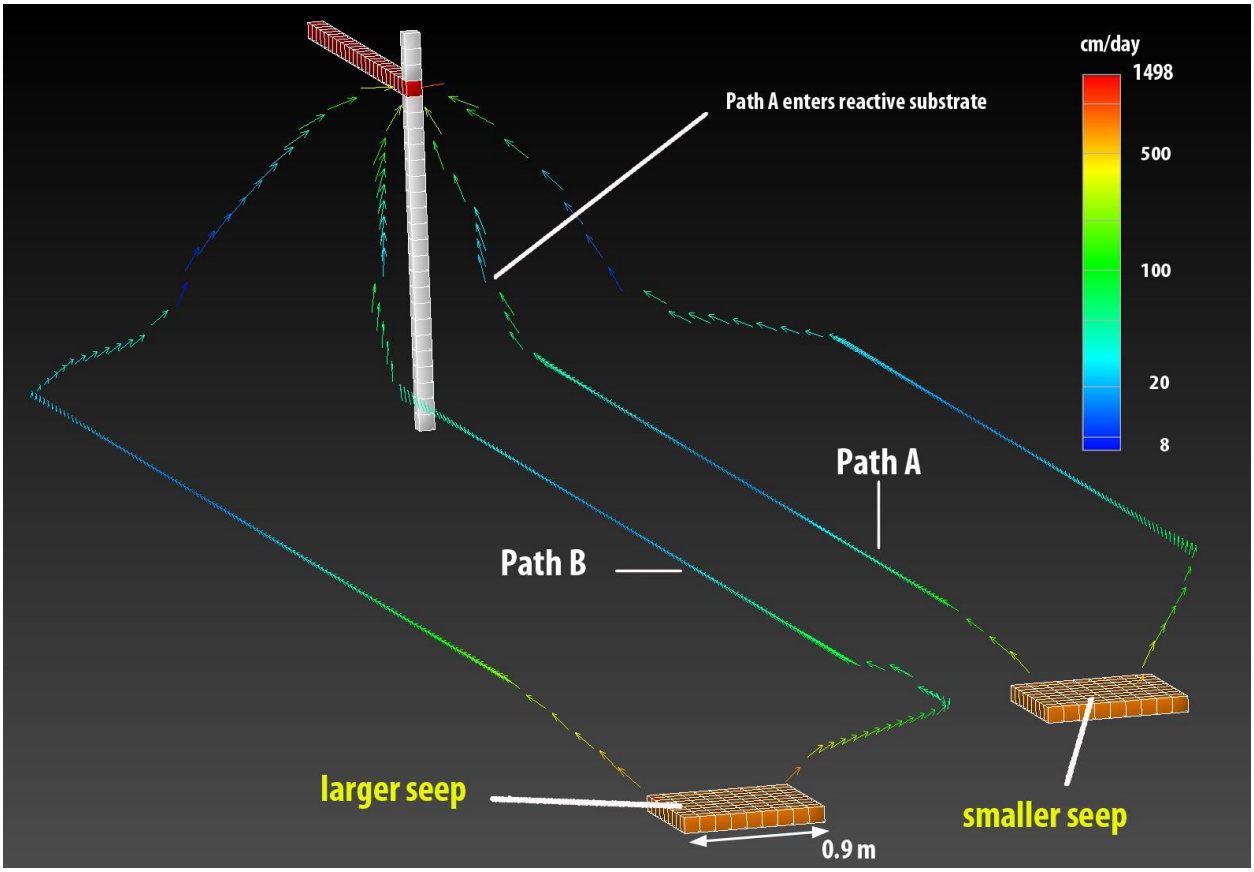

Figure 6. Three-dimensional illustration of four modeled particle paths for the Lacy North SRBC. The transit times for these particle paths ranged from 45.7 days to 71.6 days. The seep depicted in the center of the figure has a total discharge that is three times greater than the one shown on the right. The scale bar represents individual vector magnitudes (cm/day) and is logarithmic.

Lacy South

The average simulated flow rate within the Lacy South SRBC (75.0 cm/day) was over four times faster than the average flow rate within the Lacy North bioreactor, even though the average conductivity was lower in Lacy South (no woodchip layer). The higher average flow rate can be attributed to the smaller size and larger measured inflow/outflow rate of the Lacy South SRBC. Furthermore, there are consistently more zones of simulated flow having higher magnitudes within Lacy South owing to the jointed nature of the internal pipe network (Fig. 7); the total discharge into and out of the pipes is higher in the vicinity of a pipe junction.

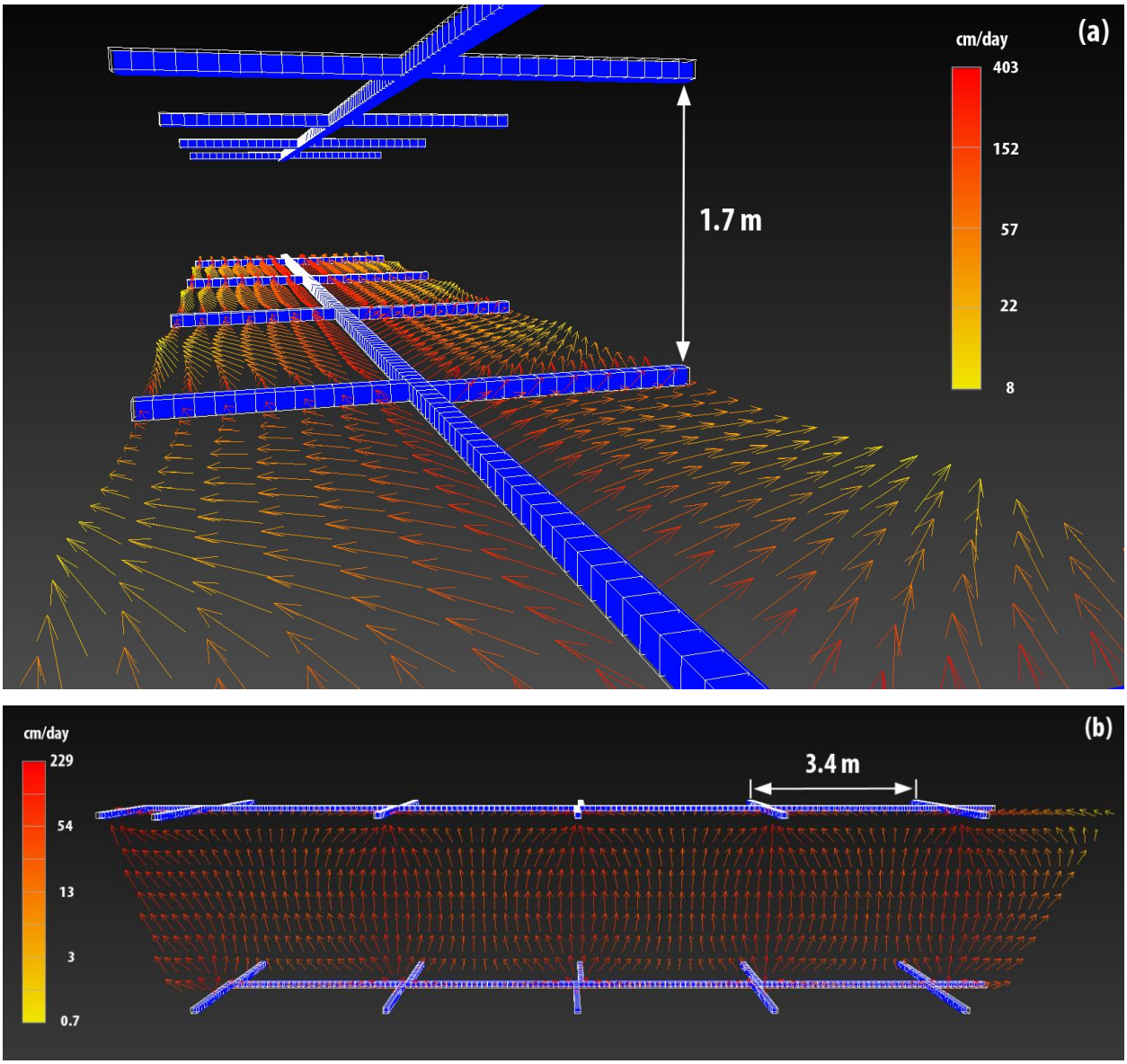

Figure 7. Three-dimensional illustrations of the Lacy South bioreactor. (a) The simulated flow field for the bottom layer (shown for every fourth vector). (b) Vertical cross section (VE = 2X) of the simulated theoretical flow. Both scale bars represent individual vector magnitudes (cm/day) and are logarithmic. For reference, the distance between the top and bottom pipe network is 1.7 m.

The minimum calculated transit time from inflow to outflow pipe within the Lacy South SRBC was 0.9 days, which was much shorter than those calculated for the Lacy North and Midwestern bioreactors. The design of Lacy South allows for a direct path from the top of the basal pipe (inflow) to the bottom face of the surface pipe (outflow) along the entire length of the bioreactor, which is where the short minimum transit times occurred. Longer transit times

develop where flux occurs along the sides of the basal pipe allowing a horizontal component of flow to exist (Figs. 7 and 8).

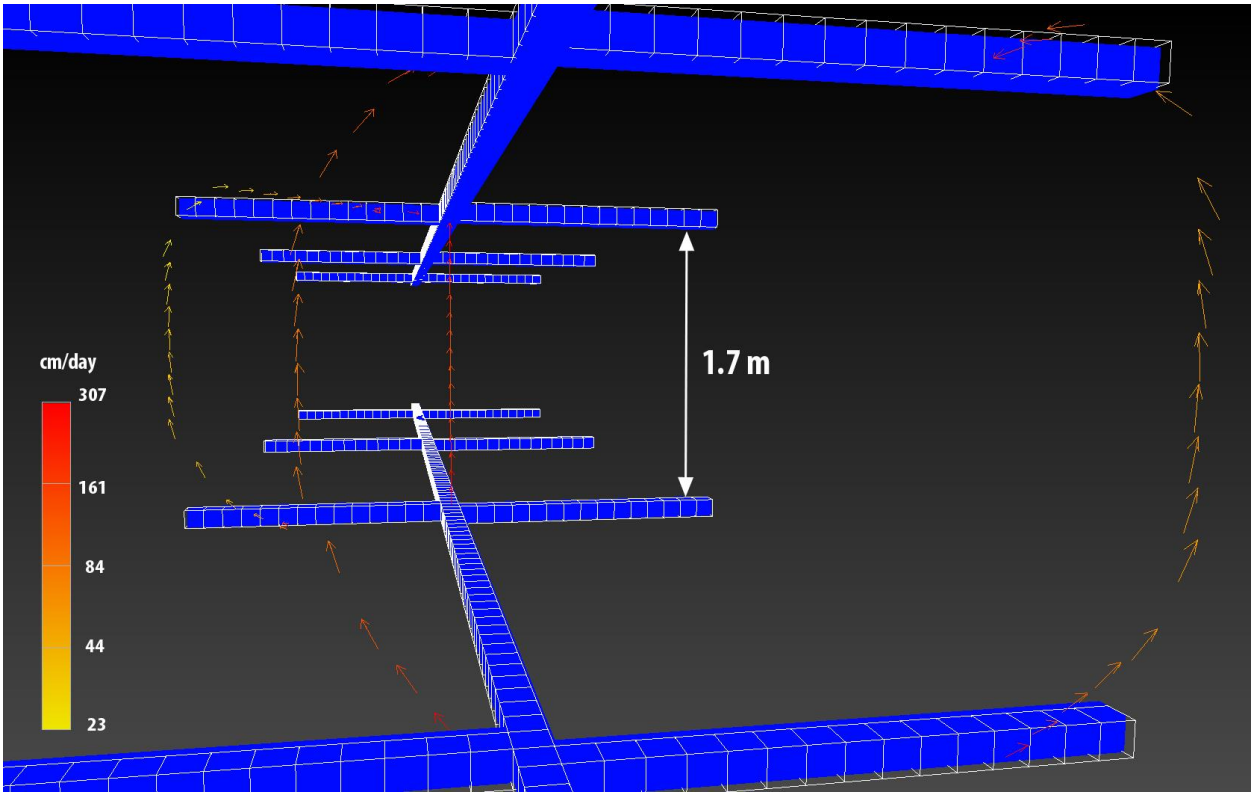

Figure 8. Three-dimensional diagram of four modeled particle paths for the Lacy South SRBC. The transit times for these particle paths ranged from 0.9 to 8.3 days. The scale bar represents individual vector magnitudes (cm/day) and is logarithmic.

Midwestern

The numerical simulation of flow through the Midwestern SRBC produced an average flow rate of 142 cm/day, the highest of all three SRBCs. This is likely a consequence of the much higher rate of discharge into and out of the bioreactor, which was about four times that of Lacy South and seven times that of Lacy North. The minimum computed transit time was only 11.9 days. This occurred along a path where the pipe network extends closest to the inflow location. It is conceivable that water could flow above the internal pipe network all the way through the reactive substrate to the outlet pipe, which would take a couple of months based on the length of the bioreactor and average flow rate. However, upon close inspection of Figure 9, this does not appear to be the case, because the simulation indicates that water is flowing toward the pipe along most of the length of the SRBC.

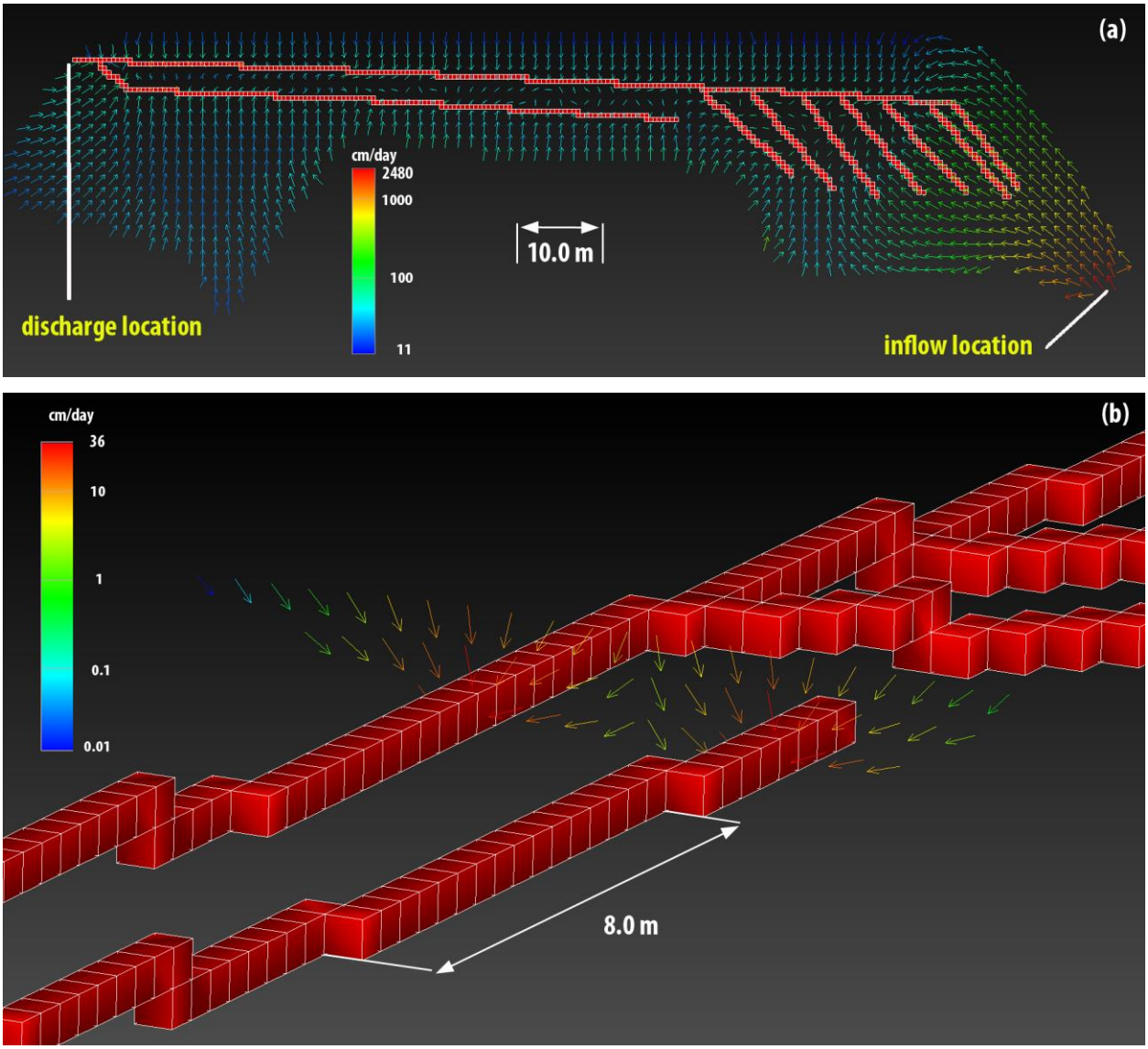

Figure 9. Map and three-dimensional diagram of the Midwestern bioreactor. (a) Flow vectors within layer 11 of the hydrogeological model. Note that near the outlet (left in this figure), the pipe network is in layer 11 and near the inflow (right in this figure), the pipe network is located 2.0 m below this layer. Note only every tenth vector is shown for clarity. (b) Vertical cross section of flow vectors midway along the pipe network. The vector scale bars in both (a) and (b) are logarithmic.

A map view of the simulated flow for an upper layer of the reactive substrate shows an influence of the pipe network, even at the inflow end where the pipes are 2 m below the surface (Fig. 9a). The highest magnitudes in this layer exist at the inflow location and near the pipe network at the outflow end of the bioreactor (where the pipe exists in the surface layer). The simulation indicated that horizontally dominant flow occurs near the inflow and out away from

the pipe network. However, near the pipe network, flow is dominantly downward toward the pipes. This downward flow occurs in both shallower and deeper parts of the bioreactor (Fig. 9b). Finally, much like the simulated transit paths within the Lacy North SRBC, a particle can take a much different path with just a slightly different starting location. Particles that enter on the left edge of the inflowing spring travel longer paths than those that enter on the right edge (Fig. 10). Overall, the longer pathways have transit times of over 22 days, whereas the shortest paths take approximately 12 days.

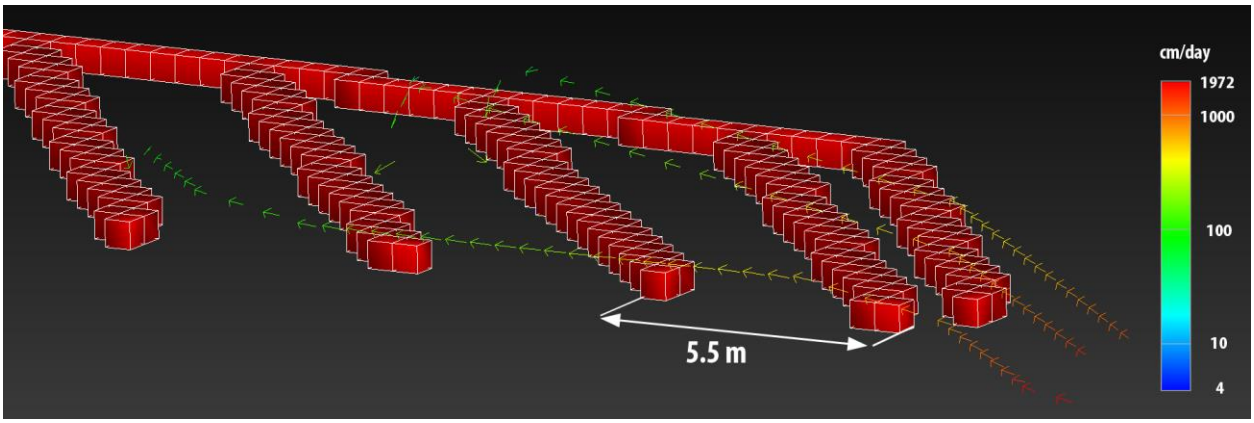

Figure 10. Three-dimensional illustration of three modeled particle paths for the Midwestern SRBC. The transit times for these particle paths ranged from 14.5 days to 15.7 days. The scale bar represents individual vector magnitudes (cm/day) and is logarithmic.

Discussion

The results of the numerical simulations show that, under conditions that existed during the initial phase of deployment, there should be different flow rates and patterns occurring in the constructed SRBCs. Those differences are based on: (1) the nature and rates of how water enters the system (surficial or basal entry), (2) the design of the internal pipe network, and (3) the overall geometry of the system. For example, extending the collection pipes within the Midwestern SRBC close to the inflow did facilitate drawing water down from the surficial spring to the deepest parts of the bioreactor. However, simulations suggest that this resulted in shorter transit times, which may contradict treatment objectives (namely, providing less time for reactions to occur). In contrast, the longest of the minimum transit times was achieved by promoting flow through the substrate in the Lacy North bioreactor (no extensive pipe network was employed). However, the inclusion of a woodchip layer undermined some of those apparent benefits.

As outlined in the companion paper (Branam et al., 2012), these systems do not appear to remain homogeneous over time. Monitoring data from the SRBCs (for the past 3 years) suggest that flow patterns changed in concert with chemical changes. For example, chemical reactions may have caused organic and mineralogic precipitation in the pore spaces of the reactive substrate at Lacy South, which, in turn, may have decreased the hydraulic conductivity and storage capacity of the porous medium. Preferential flow paths seem to have developed that undermined bioreactor performance and led to failure of the Lacy South SRBC. Tracer studies (using bromide as an indicator) at the Lacy South SRBC support the idea that the flow field did not remain uniform over time. Additional geochemical data collected within the SRBC are consistent with organic and mineralogic precipitation in the pore spaces of the reactive substrate. Inverse modeling to infer spatially variable conductivity distributions that are consistent with the tracer studies are the next step for the hydrogeologic modeling of this SRBC.

The observed flow dynamics and chemical monitoring at the Midwestern SRBC indicate a more complex hydrologic system than was foreseen in the design phase. We know from field observations that there was leakage of AMD under the berm located near the inflow; this led to a lack of flow through the outlet over extended periods of time, especially in the early months of deployment. During the wet seasons, the SRBC overfilled so that water was commonly ponded above the substrate. Under these conditions, water could have been flowing across the top of the SRBC and entering the substrate near the outflow end of the bioreactor. In such cases, the simulated transit time within the reactive substrate would be about 21 hours (as determined by particle tracking with a starting location near the pipe). Finally, extending the groundwater collection pipe network too near the AMD inflow location, particularly in the Midwestern SRBC with its higher inflow rates, resulted in shorter computed transit times within the reactive substrate than would have been accomplished otherwise. We know the role of the pipes in controlling theoretical flow paths is critical because similar results were produced even when we prescribed a variable pipe flux rate that was a function of depth of pipe below the surface (the idea being that shallower pipes receive more inflow than deeper pipes). Future modeling will simulate the system subjected to additional variable internal and external boundary conditions to help resolve complications of flow within this system.

The pipe network for Lacy South was designed to distribute the inflow lengthwise across the SRBC and along branches off the main pipe. This potentially maximizes the amount of substrate

that comes into contact with AMD, but also may result in zones exhibiting higher flow magnitudes near the pipe junctions. As indicated by the flow vectors (Figs. 7 and 8), avoiding augmented flow out near pipe junctions might provide slower flow through the bioreactor. Additionally, because mineral precipitation is likely to change the hydraulic properties over time, even a simple straightforward system like that of Lacy South may not be the optimal design. Indeed, this seems to be the case given the geochemical evidence for complete failure of this system (Branam et al., 2012). We believe more thought could be given to forcing longer flow pathways through small bioreactors like Lacy South by a combination of discontinuous impermeable layers and pipe perforations.

Conclusion

Bioreactors represent promising new technologies as passive treatment systems. The results of this study show that the details of planning the geometry and the hydrologic design of bioreactors must be carefully considered before being emplaced. Furthermore, there are great differences in the potential transit times and flow paths that result from the size and morphology and piping network of bioreactors. As models for SRBC performance continue to evolve, much attention also must be placed on how the hydraulic properties of these systems change over time, owing to chemical reactions occurring within the systems.

Acknowledgements

Funding for this project was provided through a grant from the U.S. Office of Surface Mining and a cooperative agreement with the Indiana Department of Natural Resources – Division of Reclamation. The contributions of Dr. Sally L. Letsinger (GIS analysis), John T. Haddan (field work), and Tracy D. Branam and Matthew D. Reeder (bioreactor data) are especially appreciated.

Literature Cited

Boswell, J.S. and G.A. Olyphant, 2007. Modeling the hydrologic response of groundwater dominated wetlands to transient boundary conditions: Implications for wetland restoration. Journal of Hydrology 332, 467-476. http://dx.doi.org/10.1016/j.jhydrol.2006.08.004

Branam, T.D., M.D. Reeder, and G.A. Olyphant, 2012. Theoretical versus observed hydrochemical performance of sulfate-reducing bioreactors in southwestern Indiana.

Proceedings America Society of Mining and Reclamation, 2012 pp 28-49 http://dx.doi.org/10.21000/JASMR12010028

Freeze, R.A., 1971. Three-dimensional, transient, saturated-unsaturated flow in a groundwater basin. Water Resources Research 7, 347-366. http://dx.doi.org/10.1029/WR007i002p00347.

Jacob, C.E., 1940. The flow of water in an elastic artesian aquifer. Trans. Amer. Geophys. Union part 2, 574-586. http://dx.doi.org/10.1029/TR021i002p00574.

Mualem, Y., 1976. A new model for predicting the hydraulic conductivity of unsaturated porous media. Water Resources Research 12, 513-522. http://dx.doi.org/10.1029/WR012i003p00513.

Pollock, D.W., 1988. Semianalytical computation of path lines for finite-difference models. Groundwater 26, 743-750. http://dx.doi.org/10.1111/j.1745-6584.1988.tb00425.x.

Richards, L.A., 1931. Capillary conduction of liquids through porous mediums. Physics 1, 318-333. http://dx.doi.org/10.1063/1.1745010.

Schaap, M.G., F.J. Leij, and M.T. van Genuchten, 2000. Estimation of the soil hydraulic properties. In: Looney, B.B., Falta, R.W. (Eds.), Vadose Zone: Science and Technology Solutions, vol. 1. Battelle Press, Columbus, 501-509.

van Genuchten, M.T., 1980. A closed-form equation for predicting the hydraulic conductivity of unsaturated soils. Soil Science Society of America Journal 44, 892-898. http://dx.doi.org/10.2136/sssaj1980.03615995004400050002x.